Size, flexibility, and scattering functions of semiflexible polyelectrolytes with excluded volume effects: Monte Carlo simulations and neutron scattering experiments

Luigi Cannavacciuolo,[1] Cornelia Sommer,[2] Jan Skov Pedersen,[3*,†] and Peter Schurtenberger[2,†]
[1]*Institut für Polymere, Eidgenössische Technische Hochschule, CH-8092 Zürich, Switzerland*
[2]*Department of Physics, University of Fribourg, CH-1700 Fribourg, Switzerland*
[3]*Condensed Matter Physics and Chemistry Department, Risø National Laboratory, DK-4000 Roskilde, Denmark*
(Received 3 March 2000)

We present a systematic Monte Carlo study of the scattering function $S(q)$ of semiflexible polyelectrolytes at infinite dilution, in solutions with different concentrations of added salt. In the spirit of a theoretical description of polyelectrolytes in terms of the *equivalent parameters*, namely, persistence length and excluded volume interactions, we used a modified wormlike chain model, in which the monomers are represented by charged hard spheres placed at distance *a*. The electrostatic interactions are approximated by a Debye-Hückel potential. We show that the scattering function is quantitatively described by that of uncharged wormlike chains with excluded volume effects provided that an electrostatic contribution is added to the persistence length. In addition we have studied the expansion of the radius of gyration and of the end-to-end distance. The results are in agreement with the picture outlined in the Odijk-Skolnick-Fixman theory, in which the behavior of charged polymers is described only in terms of increasing local rigidity and excluded volume effects. Moreover, the Monte Carlo data are found to be in very good agreement with experimental scattering measurements with *equilibrium polyelectrolytes*, i.e., giant wormlike micelles formed in mixtures of nonionic and ionic surfactants in dilute aqueous solution, with added salt.

PACS number(s): 61.25.Hq, 61.20.Ja, 61.12.Ex

I. INTRODUCTION

The effect of electrostatic interactions on the size and flexibility of polyelectrolytes has been the subject of intense experimental and theoretical investigations and has resulted in highly controversial results [1,2]. The persistence length of polymers and polyelectrolytes is often determined with scattering methods such as small-angle neutron (SANS) or x-ray (SAXS) scattering. The problem with most polyelectrolytes is their weak scattering power when performing such experiments, which makes it almost impossible to produce data with a sufficient accuracy over the required range of scattering vector, at low concentrations, where single-coil properties can still be resolved. To overcome these difficulties and to try to clarify some of the still open questions in the polyelectrolyte literature, it has been proposed [3,4] that solutions of polymerlike micelles ''doped'' with ionic surfactant can serve as ideal model systems for polyelectrolytes. The possibility of tuning the charge density and screening effects by adding small amounts of ionic surfactant at various salt concentrations to solutions containing giant polymerlike nonionic micelles provides us with a model having a wide range of applications.

Unfortunately, a precise determination of the flexibility from scattering data on charged wormlike micelles is problematic. First, we suffer from the lack of a conclusive and exhaustive theory for the scattering function of polyelectrolytes. Second, the often used crossover relationships or asymptotic expansions from, respectively, the coil and rod limits are too uncertain to provide a satisfactory estimate of the persistence length.

A powerful method to overcome these problems turned out to be computer simulation, which has already been applied extensively and successfully to uncharged polymers. In particular, it has been possible to simulate with Monte Carlo (MC) methods neutral semiflexible chains with excluded volume effects and to determine the scattering function in the full range of experimental interest [5]. The accuracy obtained was good enough to enable us to use the results as a fitting model for experimental SANS measurements [3,5].

Polyelectrolyte simulations are, however, as expected, more difficult and expensive in CPU time compared to neutral polymer simulations. Calculation of the electrostatic energy takes the longest time per MC step, time in principle proportional to the square of the total number of particles in the system. A complete description of polyelectrolytes in solutions with added salt should include all interactions between polyions, counterions, coions, and solvent molecules. Of course, the effects of the discreteness of these other species on the polyion are confined on a much shorter length scale than the contour length of the polyelectrolyte chains. Therefore, apart from a few basic works [6–8], it is common practice to average over the solvent molecular degrees of freedom and to treat the solvent as a dielectric continuum (continuous model). Other difficulties arise from the presence of additional length scales, not only the persistence length as in the case of neutral polymers, which produces nonuniqueness of the coarse graining procedure. For this reason most of the first MC studies were performed on different limiting situations in which one or more characteristic lengths were kept constant (e.g., unscreened Coulombic interactions, fully ionized chains, etc.). Despite those problems

*Present address: Dept. of Chemistry, Aarhus University, Langelandsgade 140, DK-800 Aarhus C, Denmark.
†Authors to whom correspondence should be addressed.

much work on polyelectrolytes has been published in the last decade. In the framework of the continuous model, publications have appeared on single chains in salt solution without explicit inclusion of counterions and coions [10–15], and with inclusion of them (primitive model) [16]. In addition, recently, also some works on many chain simulations have been published [17–20]. Stevens and Kremer have performed molecular dynamics simulation of many chain systems using a primitive model in the Debye-Hückel approximation [21] and also including the full Coulomb interactions between monomers and counterions [22–26]. Nevertheless, theoretical understanding of polyelectrolytes is still rather poor compared to that of neutral polymers. The major efforts in the simulation research have focused on the conformational properties and on the important question concerning universal behaviors of charged chains. Very few studies have been devoted to achieving a quantitative knowledge and understanding of the scattering function of such systems. This function seems to us to have at least the same importance as other quantities, which have been more actively studied, considering the fact that most of the experimental studies on polyelectrolytes have used scattering experiments and the scattering function is directly measurable. The aim of the work reported in the present article is to perform systematic large-scale MC simulations for a charged chain with excluded volume effects and to verify whether the fitting model obtained from simulations on uncharged chains [5,27] is applicable to charged systems. This would then allow one to use these model scattering functions for a quantitative analysis of experimental data in order to obtain quantities such as the persistence length L_p or equivalently the Kuhn length $b = 2L_p$. Moreover, the values of the persistence length obtained from the simulations will be compared with those achieved by SANS measurement on a system consisting of a mixture of hexaethylene glycol mono-*n*-hexadecyl-ether ($C_{16}E_6$) and a small amount of the ionic surfactant 1-hexadecane sulfonic acid ($C_{16}SO_3Na$) in very dilute solutions, with added salt (NaCl), which gives rise to charged polyelectrolytelike micelles [3,28], so called equilibrium polyelectrolytes.

II. MODEL AND SIMULATION TECHNIQUE

The model we use in the present work is based on a discrete representation of the wormlike chain (WLC) model introduced long ago by Kratky and Porod [29]. The discrete model consists of a freely rotating chain of N points separated by a distance a, and with equal valence angle θ. The chain length is therefore $L=(N-1)a$ and the intrinsic Kuhn length b $(=2L_p)$ is given by

$$b = a\frac{1+\cos\theta}{1-\cos\theta}. \tag{1}$$

The only possible movements are the rotations of the points around the connecting bonds. Excluded volume effects are reproduced by replacing the N points on the chain with N hard spheres of radius $\rho = 0.1b$ and by discarding those chain configurations with overlap of the spheres. The value of ρ has in the present work been chosen based on previous experimental observations of the local structure of wormlike micelles [30] and on the fact that the uncharged model describes the structure and excluded volume effects of both wormlike micelles and polystyrene in a good solvent [5,30]. The continuous limit in the model is obtained by letting $N \to \infty$, $a \to 0$, and $\theta \to 0$, with the constraint that L and b remain constant. This procedure has an important consequence on the criterion adopted for overlap searching. For $b/a > 5$ the radius of the spheres is larger than half the bond length and therefore it happens that some neighboring spheres overlap irrespective of chain conformations. For this reason the search for overlap in our model cannot start in the immediate neighborhood of a given monomer, as in the atomistic model, but must be further along the chain. In the simulations we have adopted the criterion to search for overlap only for spheres separated by a distance larger than $b/3$ [27]. This value allow the chains to perform a maximal bending of a semicircle for $N \to \infty$ also.

The electrostatic interactions are included by associating a charge $Z_b L/(Nb)$ with each sphere, where Z_b is the number of charges per Kuhn length. We have chosen to use 50 elementary charges per Kuhn length, which is a value that should closely correspond to the situation encountered in our experiments with polymerlike micelles [28]. We do not take into account explicitly the presence of coions and counterions in this study: the only electrostatic interactions are those between fixed charges on the polyion, screened by clouds of coions of the added salt. This is mathematically expressed by the ''crude'' approximations of the (Debye-Hückel) Coulomb interaction energy:

$$U(r) = \begin{cases} \dfrac{(Z_b L e/Nb)^2}{4\pi\epsilon_o\epsilon_r}\dfrac{e^{-r/\lambda_D}}{r} & \text{for} \quad r > 2\rho \\ \infty & \text{otherwise.} \end{cases}$$

In the above expression e is the elementary charge, ϵ_o the permittivity of vacuum, ϵ_r the dielectric constant of the solvent, and λ_D is the Debye screening length. The solvent is treated as a dielectric continuum with a dielectric constant $\epsilon_r = 78.5$ (H_2O at 25 °C), and the added salt gives rise to a screening length

$$\lambda_D = \left(\frac{\epsilon_o\epsilon_r k_B T}{2e^2 I}\right)^{1/2}, \tag{2}$$

where k_B is Boltzmann's constant, T the absolute temperature, and I the ionic strength in mol/l of the added salt. The polyion is supposed to be at infinite dilution; therefore I does not contain any contribution from the counterions of the polyion but only from the added salt ions. In order to relate the distances in the potential and the hard-core radius, we have used the Kuhn length $b = 300$ Å, which is close to the experimental value [3]. Note that for the electrostatic energy calculations we have also included interactions only between spheres separated by more than $b/3$ along the contour. This serves to avoid a divergence of the electrostatic energy in the large-N limit due to the increased contributions from nearby spheres even after renormalization of the charge. While the use of the same procedure as for the search for overlap (excluded volume interactions) in order to avoid this ''self-energy'' is somewhat arbitrary, we believe that it does not

influence the general properties of the chains. Moreover, it should be realized that this ''self energy'' does not exist in the real micellar systems considered in the experimental study due to the discreteness and finite number of their charges.

We are aware that by using the approximate Debye-Hückel potential and neglecting the explicit inclusion of the salt ions we are neglecting some important features of real polyelectrolytes in solution. Nevertheless, our philosophy was to study a few effects but in sufficiently great detail that the results can be directly compared to experimental data. This meant, for instance, minimizing the effects of having a finite N and minimizing the statistical errors. The model adopted should therefore be simple enough to allow one, with reasonable computer time, to simulate chains up to $\sim 10^4$ charged beads, and at the same time be able to reproduce the essential features of the system. To achieve an acceptable performance it is also required to use a suitable fast algorithm.

We have performed simulations for I ranging from $10^{-4}M$ to $0.1M$, and L/b from 1 to 480. In order to extrapolate all quantities of interest to the limit $N\rightarrow\infty$, for each value of L/b various simulations have been done using different values of N and n_b, ranging from 720 to 11 520 and from 3 to 192, respectively. Here n_b denotes the number of spheres per Kuhn length, $n_b=b/a$. Trial chain configurations have been generated by means of the PIVOT [31,32] algorithm. One bond i is selected at random and one of the two pieces of the chain is rotated a random angle ω_i around this bond. It has been proved that the PIVOT algorithm shows very short correlation time for self-avoiding chains [9], even when screened electrostatic interactions are included [33]. In addition we have used an algorithm due to Stellman and Gans [31] that corrects the coordinate of the points for roundoff errors, which otherwise would accumulate due to the repetitive multiplications by rotation matrices. The exponential decay of the Debye-Hückel potential allows us to introduce a cutoff length in the energy calculation [34], which has been chosen as the minimum distance such that the condition $n_b^2U(r)/(k_BT)<c_f$ is fulfilled. After a few preliminary tests it was found that the value $c_f=10^{-3}$ was the best compromise for speeding up the program and at the same time keeping the errors due the presence of the cutoff on the physical quantities (i.e., $\langle R_g^2\rangle$, $\langle D_{ee}^2\rangle$, etc.) within the statistical errors. The presence of a cutoff allows us to use the efficient zippering [34] method for calculating energies. Those tricks have the effect of speeding up the simulations considerably. The influence of the approximations introduced due to the presence of a cutoff has been investigated by using the values $c_f=10^{-4}$ and $c_f=10^{-5}$. No appreciable influence on the results was observed and the data agreed within the statistical errors. Each simulation starts with $2N$ MC steps to equilibrate the system. The statistical ensemble averages of the physical quantities of interest (such as radius of gyration, end-to-end distance, etc.) are evaluated by the usual Monte Carlo sampling. The statistical errors have been determined using a block analysis [35].

III. MATERIALS AND EXPERIMENTAL METHODS

The surfactant hexaethylene glycol mono-n-hexadecyl ether ($C_{16}E_6$) was obtained from Nikkol Ltd., Tokyo, the ionic surfactant 1-hexadecane sulfonic acid ($C_{16}SO_3Na$) was purchased from TCI, and D_2O (99% isotopic purity) was delivered from Cambridge Isotope Laboratories. The samples were obtained by first dissolving both surfactants in D_2O ($C_{16}E_6$ at 35 °C and $C_{16}SO_3Na$ at 70 °C) and mixing them together at the required concentrations and ionic strengths. The SANS measurements were performed at the instrument D22 of the ILL in Grenoble, France at a temperature of 35 °C. The initial data treatment and the data analysis were performed as described in [3].

IV. MONTE CARLO RESULTS

A. Scattering function and persistence length

The scattering function of semiflexible uncharged chains with excluded volume has been determined in a previous detailed study by Monte Carlo simulations [5]. Based on these simulations, parametrized scattering functions have been obtained and successfully used for fitting experimental neutron scattering data from polymers and polymerlike micelles [3–5,30]. The primary goal of the present work is to extend those results to charged semiflexible chains with excluded volume effects. The calculation of the scattering function was performed using an approach based on the method described by Frenkel *et al.* [36]. The chain was placed in a large cubic box and the scattering function was calculated at the reciprocal lattice points of the box. The 001, 110, and 111 directions and their equivalents were used and this gives in total 13 directions. For each of the directions (h,k,l) the scattering function is then calculated as

$$S(q_p)=\left|\sum_{j=1}^{N}\exp[-ip2\pi(hx_j+ky_j+lz_j)/L]\right|^2, \quad (3)$$

where L is the side length of the box, (x_j,y_j,z_j) is the position of the jth point, and $q_p=p(2\pi/L)(h^2+k^2+l^2)^{1/2}$ is the modulus of the scattering vector, with $p=1,2,\ldots$. The scattering functions from the different directions are averaged. Note that the use of Eq. (3) requires only $13N$ calculations as opposed to the usual N^2. In order to speed up the calculations further, the pth term in Eq. (3) was calculated using the first term ($p=1$) and the $(p-1)$st term and the addition formula for sine and cosine. The terms in the 110 and 111 directions were generated in a similar way from the terms in the 001 direction.

The typical number of generated configurations after equilibration was 5×10^5, and the scattering function was sampled stroboscopically [37] for each 500 configurations, giving a total of 1000 samples. This procedure gives an accuracy of $S(q)$ better than 2% for all chain lengths and ionic strengths used.

Examples of simulation results for the scattering functions of a chain of length $L/b=240$, and for ionic strength of $I=(5\times10^{-2})M$, $(2.5\times10^{-3})M$, $10^{-3}M$, and $10^{-4}M$ are shown in Figs. 1(a) and 1(b). The fits are performed using the previously published scattering functions for semiflexible chains with excluded volume effects [5], treating the Kuhn length $b_{tot}(n_b)$ as a fitting parameter so that the influence of electrostatic interactions on this parmameter is determined. Those functions are found to give very good fits, within the

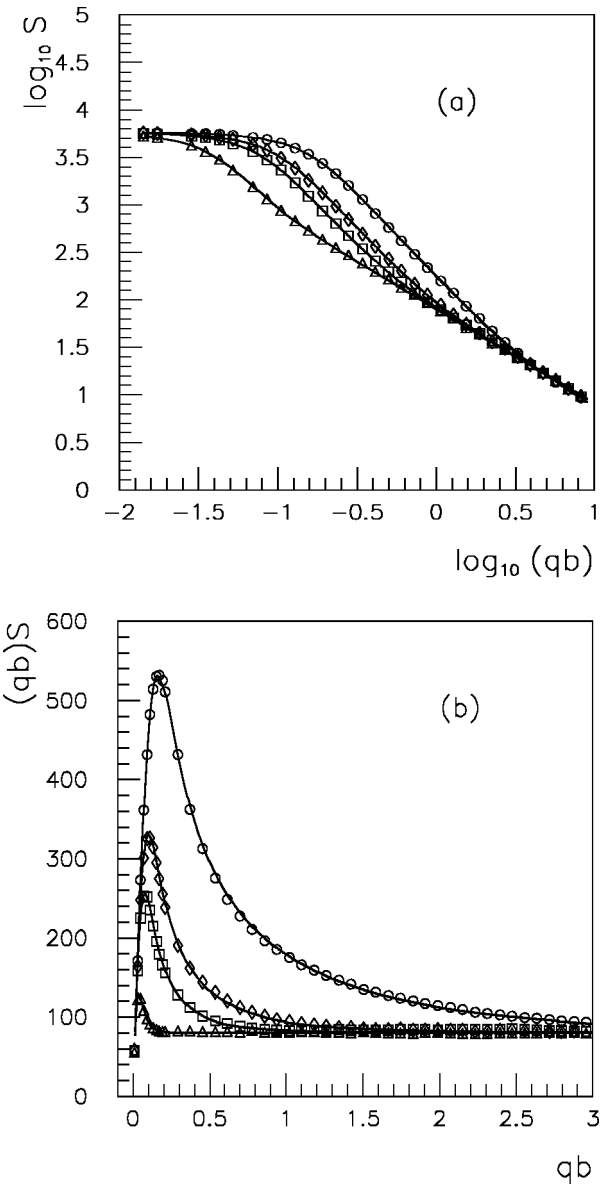

FIG. 1. (a) Scattering functions for a chain of length $L/b = 240$ and for four different ionic strengths. The fits (full lines) are performed using the wormlike chain function with excluded volume as given in [5]. Symbols: $I=10^{-4}M$ (△), $I=10^{-3}M$ (□), $I=(2.5\times10^{-3})M$(◇), and $I=(5\times10^{-2})M$(○). (b) Holtzer plot $qbS(q)$ vs qb of the scattering functions for the same simulations as in (a). Note that the point of crossover q^* shifts toward lower values of q with decreasing ionic strength, as a qualitative demonstration of the increasing stiffness of the chain.

statistical errors, of the MC data for all chain lengths and ionic strengths used. The good agreement between the fits and the simulated scattering curves is demonstrated in Fig. 1(a). Even the Holtzer plot [Fig. 1(b)], which provides us with a data representation that is particularly sensitive to small deviations in the crossover region $q^*\approx 1/L_p$, shows very good agreement at all values of L and I investigated. From these fits we obtain an effective total Kuhn length $b_{tot}(n_b)$. In order to proceed to the continuous limit, for each value of L and I we have plotted $b_{tot}(n_b)$ vs $1/n_b$. The limiting values b_{tot} have been determined from the intercept of $b_{tot}(n_b)$ vs $1/n_b$ using linear extrapolations. This procedure is displayed in Fig. 2. For $I<0.05$, b_{tot} shows a significant dependence on the chain length, clearly demonstrated in Fig. 2. This effect is also predicted in the OSF theory (Odijk, Skolnick, and Fixman) [38] by the expression

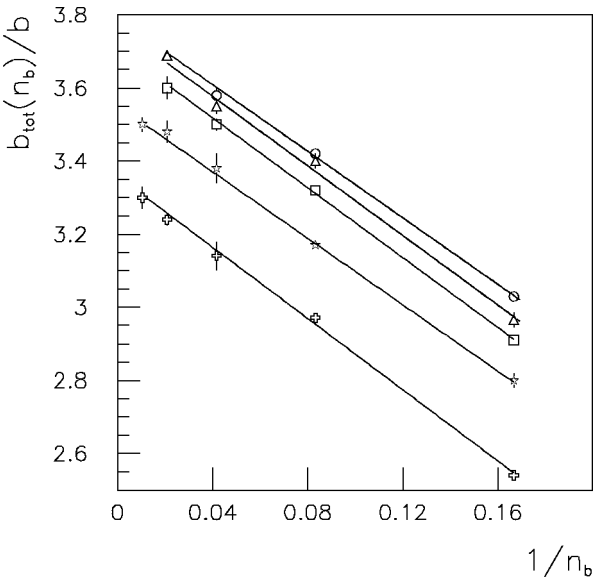

FIG. 2. Examples of the linear extrapolation of the total Kuhn length b_{tot}/b to the continuous limit, for an ionic strength of $(2.5\times10^{-3})M$ and different chain lengths (from the top, $L/b = 240, 120, 60, 30, 15$). For a given value of I, $b_{tot}(L/b,I)$ is found from the intercept of the straight line for each system size L/b. Note the strong dependence of b_{tot}/b on the chain length as soon as this becomes shorter than about 120.

$$b_{tot}(x,I)=b+b_{el}^{\infty}(I)\left[1-\frac{8}{3x}+\frac{e^{-x}}{3}\left(x+5+\frac{8}{x}\right)\right], \quad (4)$$

where $x=L/\lambda_D$, b is the *intrinsic* Kuhn length given by Eq. (1), and $b_{el}^{\infty}(I)$ is the electrostatic contribution to the Kuhn length for infinitely long chains. We tried to fit this expression to the simulation results treating $b_{el}^{\infty}(I)$ as a fit parameter. However, the expression was not able to fit the data. This is mainly because the crossover in the results shown in Fig. 3 occurs at the same L/b value for different ionic strengths, i.e., the crossover is observed to be independent of the ionic strength. The data, were, however, found to follow closely the behavior given by Eq. (4) if x was taken as $x = L/b$, enabling us to estimate $b_{tot}^{\infty}(I)=b+b_{el}^{\infty}(I)$ with good accuracy (see Fig. 3). We have not been able to find a reasonable explanation for the observed behavior and the deviations from the OSF theory. Note that after having fixed $b_{el}^{\infty}(I)$, for a given value of I, the expression can also be used for estimating $b_{tot}(L/b,I)$ for any value of the chain length. This gives us a way to assess the value for a very short chain also, where the fit of the scattering function is completely insensitive to the actual value of $b_{tot}(L/b,I)$. This will be used later in the present work in the analysis of the distribution function for the end-to-end distance.

The resulting values of the Kuhn length $b_{tot}^{\infty}(I)$ are shown in Fig. 4 as a function of the ionic strength I. Figure 4 demonstrates the increasing influence of electrostatic interactions

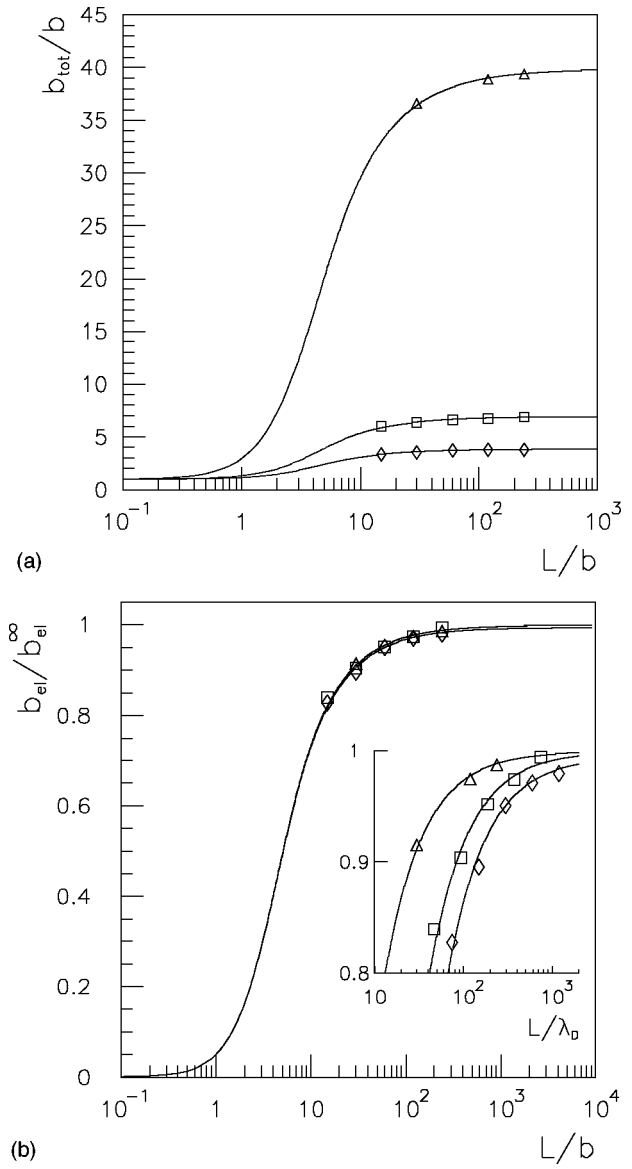

FIG. 3. (a) Total Kuhn length $b_{tot}(L/b,I)/b$ vs chain length after extrapolation of $b_{el}^{\infty}(I)/b$ by means of Eq. (4), for ionic strengths $I=10^{-4}M$ (△), $I=10^{-3}M$ (□), and $I=(2.5\times10^{-3})M$ (◇). (b) Collapse of the b_{el}/b_{el}^{∞} vs L/b data, which shows the independence of the crossover region from the ionic strength. Inset: Same quantity as before plotted vs Debye length λ_D.

on chain flexibility already apparent from the changes of the scattering curves in Figs. 1(a) and 1(b).

We can compare the simulation results with the predictions of the theoretical OSF model. The OSF theory splits the total Kuhn length into two contributions,

$$b_{tot}=b+b_{el}, \tag{5}$$

where b is the Kuhn length due to the intrinsic stiffness of the chain and b_{el} is the electrostatic contribution, which for an infinitely long chain is given by

$$b_{el}^{\infty}(I)=\frac{\lambda_B}{2}\left(\frac{\lambda_D}{d}\right)^2, \tag{6}$$

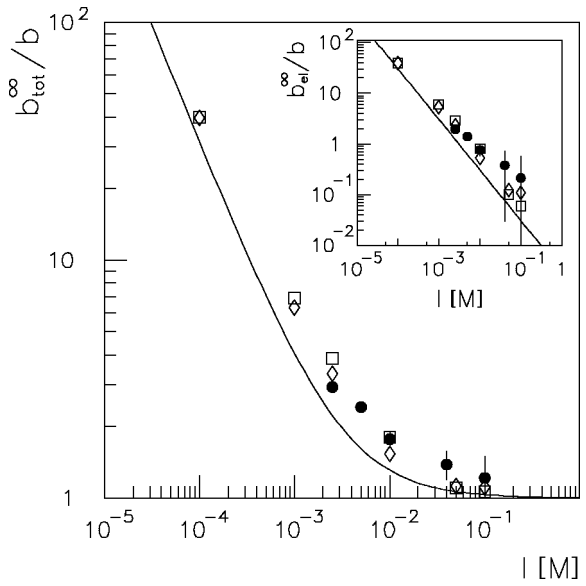

FIG. 4. Total Kuhn length $b_{tot}^{\infty}(I)/b$ vs ionic strength. Note the increase of the stiffness of the chain as the ionic strength is reduced. Inset: Electrostatic persistence length vs ionic strength. Both MC and experimental data seem to converge to OSF theory as the chain approaches the rod limit. Symbols: MC results obtained by fitting the scattering function (□) and by fitting the angular correlation function (◇); experimental SANS data (●).

where d is the distance between two neighboring charges and

$$\lambda_B=\frac{e^2}{4\pi\epsilon_o\epsilon_r k_B T} \tag{7}$$

is the Bjerrum length. In Fig. 4 the MC data are compared with the theoretical expectations of the OSF theory [38] (full line in the plot). One of the basic assumptions of OSF theory is that the polyelectrolyte is near to the rigid rod limit. If we look at the electrostatic contribution to the Kuhn length (inset in Fig. 4), we notice that for low ionic strength, i.e., for increasing stiffness of the chain, our MC results converge asymptotically to the values of OSF theory.

The MC data can also be compared with our experimental neutron scattering results on dilute mixtures of the nonionic surfactant $C_{16}E_6$ and small amounts (6% wt) of the ionic surfactant $C_{16}SO_3Na$ in a NaCl solution, which forms giant charged wormlike micelles. In the experiments the total Kuhn length was determined by least-squares fit of the experimental scattering data using the scattering function of neutral chains as the fitting model (Fig. 5). For a fixed value of the ionic strength, experiments have been performed at different concentrations of the solution. We have observed a significant dependence of the total Kuhn length on the concentration, which should be ascribed to interchain interactions [3]. The data shown in Fig. 4 are linear extrapolations of b_{tot}/b to zero concentration. The complete experimental investigation will be reported in a forthcoming article [28].

Figure 4 provides us with a qualitative verification of the previously suggested analogy between polyelectrolytes and polymerlike nonionic micelles doped with a small amount of an ionic surfactant. In these systems we can profit from the much higher scattering contrast of wormlike micelles when compared to classical polyelectrolytes, which enables us to

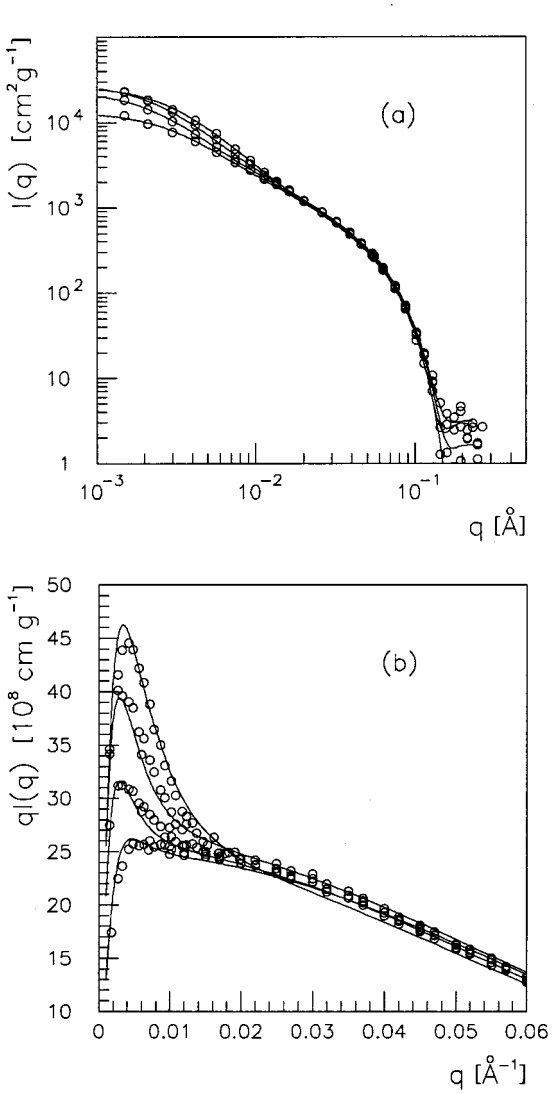

FIG. 5. (a) Scattering functions from SANS experiments with a mixture of $C_{16}E_6$ and 6 wt % of $C_{16}SO_3Na$ in D_2O with four different concentrations of NaCl [from the top, $I=10^{-1}M$, $I=10^{-2}M$, $I=(5\times10^{-3})M$, and $I=(2.5\times10^{-3})M$]. The fits (full lines) are performed using the wormlike chain function with excluded volume as given in [5]. (b) Same as in (a), but in Holtzer plot representation.

perform experiments in dilute solutions and to obtain a higher accuracy in the determination of b_{tot} from an analysis of scattering curves. We find excellent agreement between the MC simulation results and the micellar data.

Another method by which to calculate the total Kuhn length from MC data is provided by the directional angular correlation function. For the pure WLC model an exponential decay of this function is observed, and the initial decay provides an accurate estimate of L_p. As soon as excluded volume interactions are present, the exponential decay is lost, and the function exhibits a much slower decay. While we lack a detailed consistent model for the correlation function in this case, we have analyzed the correlation function using an *ad hoc* model. We will present a detailed study of this topic, including analytical results, in a future article. At the moment we only include the results in Fig. 4 in the attempt to give a more complete picture of the data analysis. Figure 4 shows that the values of b_{tot}/b obtained from $S(q)$ and from the correlation function agree quite well.

B. Radius of gyration and related quantities

The size of a chain is usually characterized by the end-to-end distance

$$\langle D_{ee}^2\rangle=\langle(\mathbf{R}_N-\mathbf{R}_1)^2\rangle, \tag{8}$$

with $\mathbf{R}_i$ being the positions of the beads, and by the radius of gyration

$$\langle R_g^2\rangle=\frac{1}{N}\sum_{i=1}^{N}\langle(\mathbf{R}_i-\mathbf{R}_{CM})^2\rangle, \tag{9}$$

where $\mathbf{R}_{CM}$ is the position of the center of mass of the chain, given by

$$\mathbf{R}_{CM}=\frac{1}{N}\sum_{i=1}^{N}\mathbf{R}_i. \tag{10}$$

We have calculated the mean square values of the radius of gyration $\langle R_g^2\rangle$, of the end-to-end distance $\langle D_{ee}^2\rangle$, of the end-to-middle distance $\langle D_{em}^2\rangle$, and of the distance between two inner points $\langle D_{ii}^2\rangle$ situated at $L/4$ and $3L/4$ along the chain, as well as the respective distribution functions (data for the last two quantities are not shown in the present paper). For fixed values of L/b, the effects of the finite number of points on $\langle R_g^2\rangle$ and $\langle D_{ee}^2\rangle$ were taken into account by making a linear extrapolation of those quantities vs $1/n_b$ to $1/n_b\rightarrow0$. The data were found to be fitted very well by a straight line, and the effects of finite size were less than 1% for all the simulations.

The conformation of a chain can be characterized by means of the shape parameter $G=\langle D_{ee}^2\rangle/\langle R_G^2\rangle$, which varies from 6 (ideal chain) to 12 (rigid rod). Figure 6 shows the values obtained from the MC simulations for the shape parameter of uncharged and charged chains with three different ionic strengths. The simulations are found, as expected, to cover almost the entire range from coil-like to rodlike chains. The change of shape of the curves with respect to the uncharged one, which is particularly pronounced at low salt concentrations, is a consequence of the chain length dependence of the electrostatic persistence length, which has been described in the previous section (see, in particular, Fig. 3). At low salt concentrations, short chains are hindered from becoming a rigid rod by the simultaneous loss of persistence. On reducing the chain length, a point is reached where the effect of the electrostatic persistence length becomes completely negligible when compared to the intrinsic stiffness. In Fig. 6 this corresponds to the point where the different curves merge into a single one. From that point on, the effect of the presence of charges disappears completely: all systems behave as if uncharged when the chain length is reduced. In the region where b_{el} varies sensitively with L the chains exhibit a kind of ''anomalous'' deformation, and, as we will see in the next section, the fitted exponents of the end-to-end distribution function also show an ''anomalous'' behavior. These effects can be accounted for by plotting G vs L/b_{tot} instead [Fig. 6(b)], and we see that all data points collapse

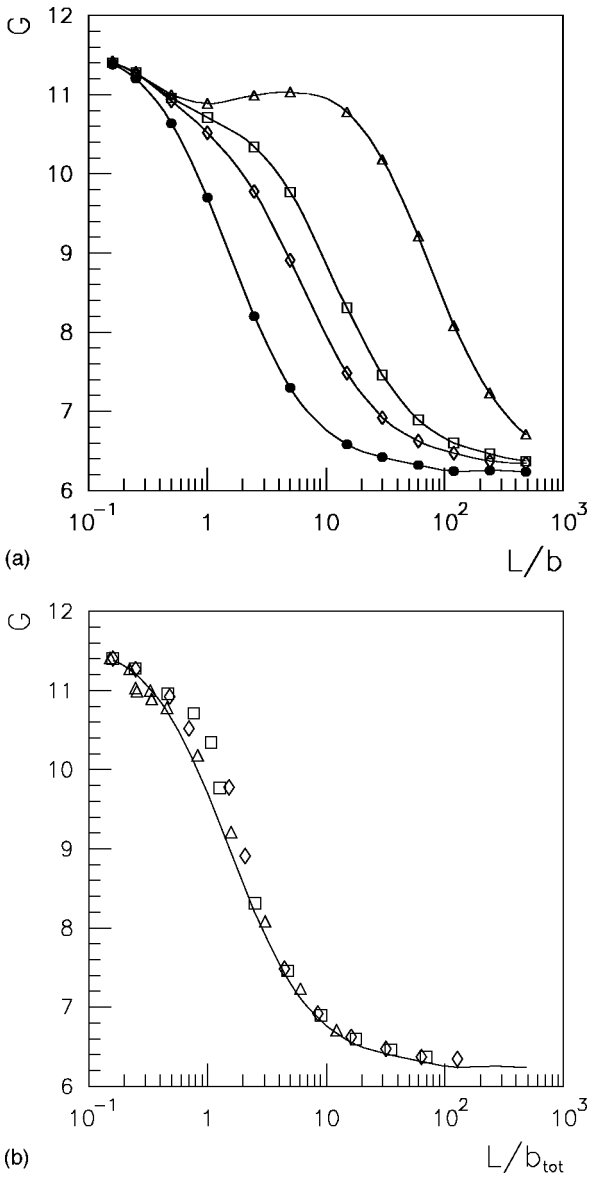

FIG. 6. (a) Shape parameter G vs chain length L/b. From left to right: uncharged system, and charged system with ionic strength $I=(2.5\times10^{-3})M$, $I=10^{-3}M$, and $I=10^{-4}M$. Note the effect of the decreasing electrostatic persistence length for the charged systems when L/b is in the range $\simeq0.5$ to $\simeq20$. The effect is particularly evident for $I=10^{-4}M$, producing a deformation in the corresponding curve. (b) Shape parameter G vs rescaled chain length L/b_{tot} for the same data shown in (a). The data for the neutral chains are shown as a full line.

onto a master curve. Some deviations can still be observed for a few points at $I=(2.5\times10^{-3})M$, $10^{-3}M$, and $1\lesssim L/b\lesssim5$. We think that under these conditions Eq. (4) slightly underestimates b_{tot}.

Excluded volume effects and electrostatic interactions lead to a significant swelling of the chain dimensions compared with the situation of semiflexible chains in θ solvent. The increase of, e.g., the radius of gyration with respect to the ideal case is often expressed in terms of the *expansion factor* [39]

$$\alpha_g^2=\frac{\langle R_g^2\rangle}{\langle R_{g,0}^2\rangle}, \tag{11}$$

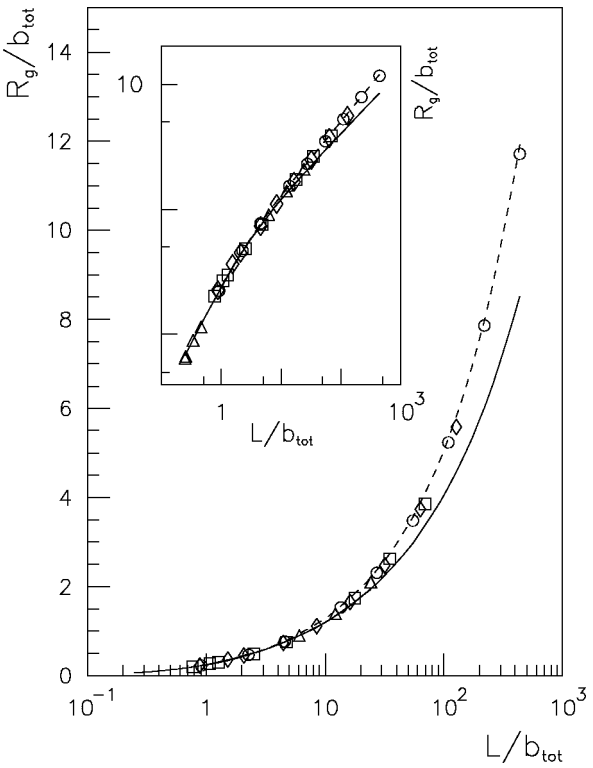

FIG. 7. Rescaled values of the radius of gyration from MC simulations vs rescaled chain length, for four different ionic strength. Full line: theoretical values for an ideal chain. Broken line: values for a neutral chain with excluded volume interactions. Symbols: same as in Fig. 1(a).

where the zero subscript denotes the value for the noninteracting chains. Analogous quantities can be defined also for D_{ee}, D_{em}, and D_{ii}. In a previously published work [27] the dependence of R_g, D_{ee}, D_{em}, and D_{ii} on chain length was analyzed in detail for neutral systems with excluded volume interactions, by MC simulations. In order to apply the simulation results to the analysis of experimental data, the authors have found the following empirical expression for the expansion factor:

$$\alpha^2(x)=\left[1+\left(\frac{x}{c_1}\right)^2+\left(\frac{x}{c_2}\right)^3\right]^{\epsilon/3}, \tag{12}$$

where $x=L/b$, to fit the MC data in the full range of L/b (up to $\approx18\,000$) very well. The parameters c_1 and c_2 are different for different quantities, e.g., R_g, D_{ee}, D_{em}, and D_{ii}, whereas ϵ is an effective scaling exponent $\epsilon=0.170$. The values of the parameters in Eq. (12) obtained for the expansion factor of the radius of gyration are

$$c_1=3.12, \quad c_2=8.67. \tag{13}$$

The basic idea in OSF theory is to treat interaction between neighboring charges as a local effect that produces an increase in the persistence length of the chain, and to incorporate those between charges located far apart along the chain into excluded volume effects. Moreover, these two effects are assumed to be uncorrelated. Using these *equivalent pa-*

rameters, one can then try to use the well developed theory of (neutral) polymers in the analysis of data from polyelectrolytes.

To test the OSF approach we have plotted in Fig. 7 the values obtained from the simulations for the dimensionless quantities R_g/b_{tot} vs chain length L/b_{tot}, where $b_{tot}=b+b_{el}$, b, and b_{el} being the intrinsic and electrostatic Kuhn lengths. It is interesting to observe that the data follow one common curve, which suggests a universal behavior. The data are compared with R_g of an ideal wormlike chain with Kuhn length b_{tot} and with the same rescaled contour length (full line in the plot). The values of b_{tot} are those obtained from the scattering function as described in Sec. IV A. The radius of gyration of such a chain, which we will call the *ideal equivalent chain*, has been calculated by means of the Benoit-Doty [40] relation

$$\langle R_{g,0}^2\rangle=\frac{1}{6}Lb-\left(\frac{b}{2}\right)^2+\frac{b^3}{4L}\left(1+\frac{b}{2L}(e^{-2L/b}-1)\right). \tag{14}$$

The full line in the plot contains therefore only the local effects of the electrostatic interactions, i.e., it takes into account only the increase of the persistence length but not the excluded volume effects. These latter are finally considered by computing the quantities $R_{g,0}\alpha_g$, with α_g given by Eq. (12) and the corresponding values for the parameters given in Eq. (13) (broken line in the plot). The effect of excluded volume can clearly be seen. On increasing L/b_{tot} the points move away from the ideal equivalent behavior and follow the behavior given by Eq. (12). This result demonstrates the consistency of our simulation results with the general OSF approach. Moreover, it shows that it is possible to determine b_{tot} from experimental data provided that one uses the appropriate expansion factor in order to incorporate excluded volume and long range electrostatic interactions effects. It is interesting to note that we find that the data follow closely the behavior predicted by the expansion factor [Eqs. (12) and (13)] for uncharged chains.

We can try to understand the observed universal behavior found for R_g on the basis of the expansion factor perturbation theory of Yamakawa, Stockmayer, and Shimada (YSS) [41]. This theory has already been used for uncharged systems with excluded volume effects [27]. In that case the results were found to follow, at least for $L/b\lesssim 1000$, the theoretical behavior expected, and a value of 0.3 was established for the (reduced) binary cluster integral (BCI).

According to YSS theory the expansion factor of the radius of gyration is given by

$$\alpha^2=\left[1+10\tilde{z}+\left(\frac{70}{9}\pi+\frac{10}{3}\right)\tilde{z}^2+8\pi^{3/2}\tilde{z}^3\right]^{2/15}\times[0.933+0.67\exp(-0.85\tilde{z}-1.39\tilde{z}^2)], \tag{15}$$

where

$$\tilde{z}=3/4K(l)z, \tag{16}$$

$K(l)$ is a complicated function of the chain length $l=L/b_{tot}$, which cannot be expressed in closed form, and

$$z=(3/2\pi)^{3/2}Bl^{1/2} \tag{17}$$

where B is the reduced BCI. All lengths are in reduced units, i.e., in units of b_{tot}. A numerical expression for $K(l)$ is provided by [42]

$$K(l)=\begin{cases}\dfrac{4}{3}-\dfrac{2.177}{l^{1/2}}+\dfrac{7}{6l} & \text{for} \quad l>6\\ l^{-1/2}\exp\left(-\dfrac{6.611}{l}+0.9198+0.035\,16l\right) & \text{for} \quad l\leqslant 6.\end{cases} \tag{18}$$

If we apply the YSS theory to the charged system, and rescale all lengths by b_{tot}, the universal behavior shown in Fig. 7 is achieved if the reduced BCI is the same at all ionic strengths. This means that if we denote the BCI of the uncharged and charged systems, respectively, by β_0 and β in units of a ''real'' volume, we expect

$$\frac{\beta}{\beta_0}=\left(\frac{b_{tot}}{b}\right)^3. \tag{19}$$

The validity of Eq. (19) cannot be established rigorously on the basis of the existing theories for the binary cluster integral and in our opinion should be the objective of further, deeper investigations.

C. Distribution function for the end-to-end distance

In Fig. 8(a) we report the distribution functions of the end-to-end distance for a chain of length $L/b=240$ and four different values of the ionic strength. As the ionic strength is reduced the distribution functions become narrower and the maximum approaches the mean value $D_{ee}=(\langle D_{ee}^2\rangle)^{1/2}$. Such behavior is a result of the stretching of the chain due to the increasing electrostatic repulsion as a consequence of the decreasing screening part of the potential. The effect is even more evident in Fig. 8(b), which displays the same data but for a shorter chain ($L/b=15$). It is instructive to note the corresponding range in rescaled length L/b_{tot}, which for Fig. 8(a) is $6.1\leqslant L/b_{tot}\leqslant 216.2$, and for Fig. 8(b) is $0.45\leqslant L/b_{tot}\leqslant 13.6$.

The fits shown in the figure were obtained using a function proposed by Mazur [43]:

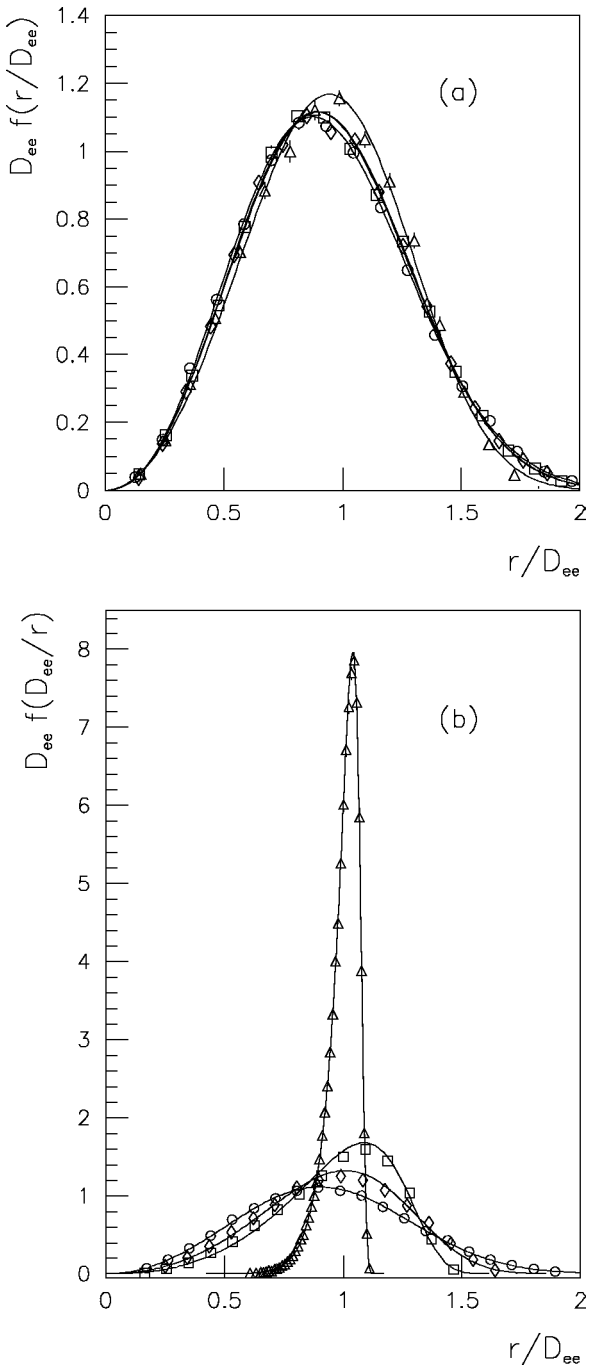

FIG. 8. (a) Distribution functions for the end-to-end distance for a chain length $L/b=240$, for different ionic strengths. Fits are done using the Mazur function [43]. Symbols: same as in Fig. 1(a). (b) Same as in (a) but for a chain length $L/b=15$. At decreasing ionic strength the chain is more and more stretched. This corresponds to distribution functions that are more narrower and whose maximum approaches the corresponding mean value.

$$f(r)=Cr^{s}e^{-(r/\sigma)^{t}}, \tag{20}$$

where C is a normalization constant, s and t are parameters that determine the shape of the distribution, and $\sigma^2=\langle D_{ee}^2\rangle\Gamma[(s+1)/t]/\Gamma[(s+3)/t]$, where $\Gamma(x)$ is the gamma function. This function turned out to give good fits for almost all the values of L/b and I used in the simulations. There are

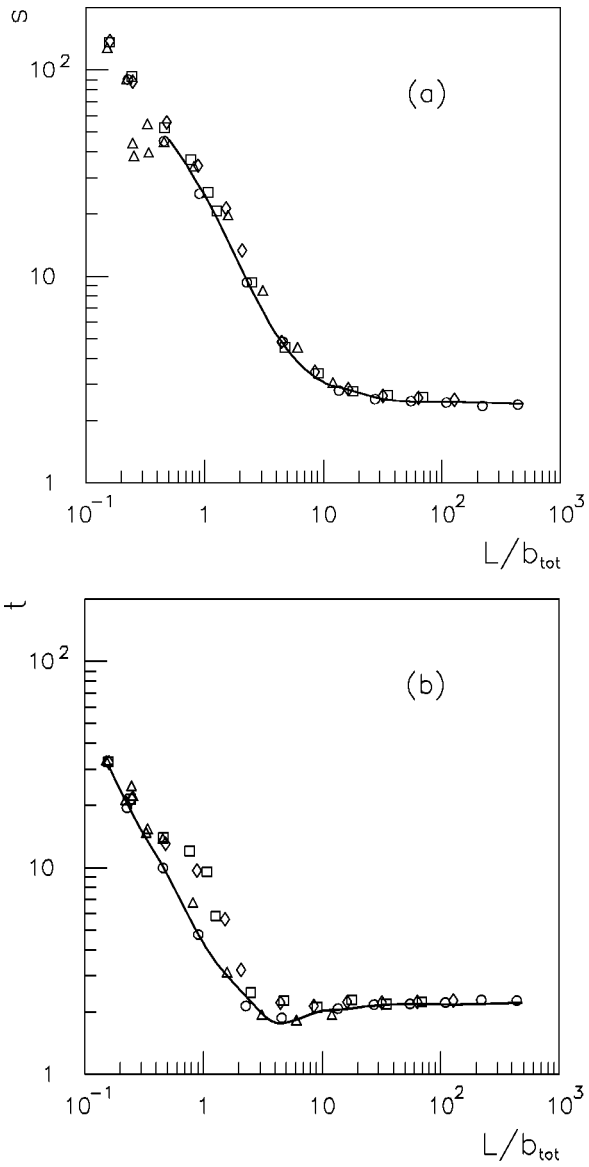

FIG. 9. Values of the fit parameters s (a) and t (b) vs rescaled chain length. Full lines: respective values of s and t for uncharged system as obtained in [27]. Symbols: same as in Fig. 1(a).

nevertheless a few exceptions, as, for instance, the data for $I=10^{-4}M$ in Fig. 8(a) and $I=(2.5\times10^{-3})M$ and $10^{-3}M$ in Fig. 8(b). We have found that Eq. (20) ''fails'' for chains having G in the range from about 7.5 to 8.5, that is, for chains that are already relatively stiff but do not yet behave as rods. The results for the exponents s and t are plotted in Fig. 9 against the rescaled chain length L/b_{tot}. For short chains, the values of b_{tot} used have been obtained by the method described in Sec. IV A. The two lines correspond to the s and t values of uncharged chains already obtained in a previous study [27]. We find that, if we rescale all the lengths, the values of s and t also collapse onto a single curve, which coincides with the curve describing the uncharged system. This is not the case for those points lying in the region where the electrostatic persistence length is a strongly varying function of the chain length as described in the preceding section.

V. CONCLUSIONS

We have performed a Monte Carlo simulation study of a self-avoiding semiflexible chain model with electrostatic interactions described by a Debye-Hückel-type potential. Simulations were performed as a function of chain length and ionic strength of the solvent. Care was taken to extrapolate all derived quantities to the continuous limit of the chain. The scattering functions, sampled during the simulations, were analyzed and the total Kuhn length, which includes the effects of electrostatic interactions, was determined. The results are in excellent agreement with the Kuhn length determined for charged wormlike micelles under similar conditions as used in the simulations. Both sets of results are in reasonable agreement with the classical OSF theory; however, the observed Kuhn length is slightly larger than predicted.

The radius of gyration and end-to-end distance, as well as the distribution of the latter, were also sampled during the simulations. Plotting the radius of gyration as a function of the contour length in units of the total Kuhn length makes the data for different ionic strengths collapse on the same curve. This universal behavior is in fact the same as that found for neutral semiflexible chains with excluded volume interactions. This suggests that the binary cluster integral, which describes the strength of the interactions, scales with the cube of the total Kuhn length. The distribution functions for the end-to-end distance were analyzed with the Mazur distribution function. The two characteristic parameters of this function were plotted versus the contour length in units of the total Kuhn length: The data were found to display universal behavior for chains longer than twice the total Kuhn length, and again the data coincide with the results for neutral semiflexible chains.

There are two main conclusion from this analysis of Monte Carlo simulation results and experimental results for charged wormlike chains. (i) The electrostatic contribution to the Kuhn length is very well described by a model with semiflexible hard-sphere chains with an added Debye-Hückel potential. (ii) The behavior of the chains is universal when the contour length is taken in units of the total Kuhn length. The latter conclusion has the implication that the electrostatic interactions change the local properties, i.e., the Kuhn length, and the long range interactions, so that the behavior in many respects is equivalent to that of a neutral self-avoiding chain with a reduced binary cluster integral of 0.3.

In the present work a so-called continuous model was used, in which the the atomic structure of the chain as well as the solvent is neglected and an effective potential is used. Despite the fact that the use of such a continuous model for simulation of polyelectrolyte chains has been questioned by groups who conducted MC simulations in which they explicitly accounted for counterions and co-ions (primitive model), we found excellent quantitative agreement between the scattering functions and the Kuhn length obtained from our MC simulations and the experimental data obtained with equilibrium polyelectrolytes. It is clear that our data have been obtained under conditions where the approximations made should be appropriate. However, it is also clear that we are now in a position to compare experimental scattering data of a quality far superior to those obtained with classical polyelectrolytes with simulated scattering functions. It will now be very interesting to systematically exploit doped wormlike micelles as model systems for polyelectrolytes in order to fully investigate the effects of electrostatic interactions on the single- and many-chain scattering functions, and thus help to solve some of the most puzzling open questions in this field. Interchains interactions, which are not considered here, will be treated in a forthcoming article.

A major drawback in establishing doped nonionic micelles as model polyelectrolytes is still caused by the limiting range of ionic strength values where stable micellar solutions exist. This is caused by the variation of the Kraft temperature of the ionic surfactant at low I values, which restricts our measurements to $I \geqslant (2.5\times 10^{-3})M$. However, we are currently establishing alternative conditions that would allow measurements at lower values of I, where we enter the interesting regime $b_{tot}/b \gg 1$.

ACKNOWLEDGMENTS

The support of the Swiss National Science Foundation (Grant No. 20-53381.98 and 20-46627.96) is gratefully acknowledged. We thank Dr. S. U. Egelhaaf for his help with the SANS measurements. The neutron scattering experiments were performed on the instrument D22 of the Institut Laue-Langevin in Grenoble.

[1] See, for example, H. Dautzenberg, W. Jaeger, J. Kötz, B. Philipp, Ch. Seidel, and D. Stscherbina, *Polyelectrolytes* (Hanser Publishers, Munich, 1994).

[2] *Macro-ion Characterization: From Dilute Solution to Complex Fluid*, Vol. 548 of ACS Symposium Series, edited by K. S. Schmitz (ACS, Washington, DC, 1994).

[3] G. Jerke, J. S. Pedersen, S. U. Egelhaaf, and P. Schurtenberger, Langmuir **14**, 6013 (1998); C. Sommer, L. Connavaceivolo, S. V. Egelhaaf, J. S. Pedersen, and P. Schurtenberger, Prog. Colloid Polym. Sci. **115**, 347 (2000).

[4] L. J. Magid, J. Phys. Chem. B **102**, 4064 (1998).

[5] J. S. Pedersen and P. Schurtenberger, Macromolecules **29**, 7602 (1996).

[6] E. Clementi, J. Phys. Chem. **74**, 4426 (1985).

[7] E. Clementi and G. C. Lie, in *Supercomputer Research in Chemistry and Chemical Engineering*, Vol. 353 of ACS Symposium Series, edited by K. F. Jensen and D. G. Truhlar (ACS, Washington, DC, 1987), p. 237.

[8] D. Levesque and J. J. Weiss, in *Monte Carlo Method in Condensed Matter Physics*, Vol. 71 of *Topics in Applied Physics*, edited by K. Binder (Springer, Berlin, 1995), p. 121.

[9] N. Madras and A. D. Sokal, J. Stat. Phys. **50**, 109 (1988).

[10] S. L. Carnie, G. A. Christos, and T. P. Creamer, J. Chem. Phys. **89**, 6484 (1988).

[11] S. L. Carnie, G. A. Christos, and T. P. Creamer, Macromolecules **25**, 1121 (1992).

[12] H. H. Hooper, H. W. Blanch, and J. M. Prausnitz, Macromolecules **23**, 4820 (1990).

[13] C. H. Reed and W. F. Reed, J. Chem. Phys. **94**, 8479 (1991).
[14] U. Micka and K. Kremer, J. Phys.: Condens. Matter **8**, 9463 (1996).
[15] U. Micka and K. Kremer, Europhys. Lett. **38**, 279 (1997).
[16] S. L. Carnie and G. A. Christos, J. Chem. Phys. **92**, 7661 (1990).
[17] A. J. Hasalam, G. Jackson, T. C. B. McLeish, J. Chem. Phys. **111**, 416 (1999).
[18] M. Ullner, G. Staikos, and D. N. Theodorou, Macromolecules **31**, 7921 (1998).
[19] H. Schafer and C. Seidel, Macromolecules **30**, 6658 (1997).
[20] G. A. Christos and S. L. Carnie, Chem. Phys. Lett. **172**, 249 (1990).
[21] M. J. Stevens and K. Kremer, J. Phys. II **11**, 1607 (1996).
[22] M. J. Stevens and K. Kremer, J. Chem. Phys. **103**, 1669 (1995).
[23] M. J. Stevens and K. Kremer, in *Macro-Ion Characterization: From Dilute Solution to Complex Fluid* (Ref. [2]), p. 57.
[24] M. J. Stevens and K. Kremer, Phys. Rev. Lett. **71**, 2228 (1993).
[25] M. J. Stevens and K. Kremer, Macromolecules **26**, 4717 (1993).
[26] K. Kremer, B. Dunweg, and M. J. Stevens, Physica A **194**, 321 (1993).
[27] J. S. Pedersen, M. Laso, and P. Schurtenberger, Phys. Rev. E **54**, R5917 (1996).
[28] C. Sommer, L. Cannavacciuolo, S. U. Egelhaaf, J. S. Pedersen, and P. Schurtenberger (unpublished).
[29] O. Kratky and G. Porod, Rev. Trav. Chim. **68**, 1106 (1949).
[30] G. Jerke, J. S. Pedersen, S. U. Egelhaaf, and P. Schurtenberger, Phys. Rev. E **56**, 5772 (1997); A. Stadner, O. Glatter, and P. Schurtenberger, Langmuir **16**, 5345 (2000); J. S. Pedersen, S. U. Egelhaaf, and P. Schurtenberger, J. Phys. Chem. **99**, 1299 (1995).
[31] S. D. Stellman and J. P. Gans, Macromolecules **5**, 516 (1972).
[32] C. Seidel, H. Schlaken, and I. Müller, Macromol. Theory Simul. **3**, 333 (1994).
[33] C. Seidel, Ber. Bunsenges. Phys. Chem. **100**, 757 (1996).
[34] S. D. Stellman, M. Froimowitz, and P. J. Ganz, J. Comput. Phys. **7**, 178 (1971).
[35] H. Flyvbjerg and H. G. Petersen, J. Chem. Phys. **91**, 461 (1989).
[36] D. Frenkel, R. J. Vos, C. G. de Kruif, and A. Vrij, J. Chem. Phys. **84**, 4625 (1986).
[37] G. A. Christos and S. L. Carnie, J. Chem. Phys. **91**, 439 (1989); **92**, 7661 (1990).
[38] T. Odijk, J. Polym. Sci., Polym. Phys. Ed. **15**, 477 (1977); J. Skolnick and M. Fixman, Macromolecules **10**, 944 (1977).
[39] H. Yamakawa, *Modern Theory of Polymer Solutions* (Harper & Row, New York, 1971).
[40] H. Benoit and P. Doty, J. Phys. Chem. **57**, 958 (1953).
[41] H. Yamakawa and W. H. Stockmayer, J. Chem. Phys. **57**, 2843 (1986); J. Shimada and H. Yamakawa, *ibid.* **85**, 591 (1986).
[42] T. Arai, F. Abe, T. Yoshizaki, Y. Einaga, and H. Yamakawa, Macromolecules **28**, 3609 (1995).
[43] J. Mazur, J. Res. Natl. Bur. Stand., Sect. A **69**, 355 (1965); J. Chem. Phys. **43**, 4354 (1965).